

DODECANOIC ACID INDUCES OXIDATIVE STRESS-MEDIATED DEATH IN LIVER CANCER CELLS THROUGH THE MITOCHONDRIAL PATHWAY

Xiaoguang CHEN¹ , Qionxia LV¹ , Haonan LI¹ , Zhe WANG¹ 

¹Animal Science and Technology School, Henan University of Science and Technology, Kaiyuan Avenue, Luoyang, China

Corresponding author:

Xiaoguang Chen
cxguang1015@126.com

How to cite: CHEN, X., et al. Dodecanoic acid induces oxidative stress-mediated death in liver cancer cells through the mitochondrial pathway. *Bioscience Journal*. 2024, **40**, e40036. <https://doi.org/10.14393/BJ-v40n0a2024-71135>

Abstract

It has been reported that dodecanoic acid (DDA) exerts anticancer effects on cancers of the reproductive system and digestive system. However, its role in liver cancer and its potential mechanism have rarely been defined. Therefore, in this study, Hepa 1-6 liver cancer cells were incubated with different DDA concentrations (0.1, 0.3, 0.5, 1, 2, 4 mM) for 24, 48 and 72h, and the optimal DDA concentration was determined via a cell viability test. Apoptosis and cell cycle distribution were determined by flow cytometry. SOD activity, mitochondrial membrane potential (MMP), ATP, GSH and ROS levels were measured by commercial assay kits; Bcl-2, Bax and Caspase-3 protein levels were analyzed by western blot. The results showed that 0.5 mM DDA decreased cell viability in a time-dependent manner, so this concentration was used to investigate how DDA leads to Hepa 1-6 cell apoptosis. After treatment with DDA, a significant, time-dependent increase in the cell apoptotic rate was detected despite the accumulation of S-phase cells. The increased ROS levels and decreased GSH levels and SOD activity in DDA-treated cells indicated the occurrence of oxidative stress. Mitochondrial dysfunction was evidenced by a decreased MMP and reduced ATP levels. Cell apoptotic death via the mitochondrial pathway was indicated by a reduced Bcl-2/Bax ratio and increased caspase-3 protein levels. It can be concluded that DDA can effectively trigger liver cancer cell death by inducing oxidative stress and disrupting mitochondrial function. These findings provide new insight into the potential mechanism of action of DDA in liver cancer.

Keywords: Cell apoptosis. Dodecanoic acid. Liver tumor. Medium chain fatty acid. Oxidative stress.

1. Introduction

Liver cancer is a highly prevalent malignancy worldwide and ranks sixth in cancer incidence and second in mortality among highly lethal tumors, with more than half of the total deaths occurring in China (Fu and Wang 2018). The etiologies of liver cancer are diverse, with obesity, chronic liver disease and alcohol consumption being the main risk factors (Colombo and Lleo 2018; Cowppli-Bony et al. 2019). For instance, obesity leads to fat accumulation in the liver, which may initiate nonalcoholic fatty liver disease (NAFLD), causing inflammation and fibrosis that can further develop into liver cancer (Polyzos et al. 2019). Studies have shown that the risk of liver cancer development in NAFLD patients is significantly increased, which may be associated with mechanisms such as insulin resistance, chronic inflammation and oxidative stress (Petersen and Shulman 2018; Gabbia et al. 2021). Additionally, chronic liver diseases such as hepatitis C and B also substantially contribute to liver inflammation, fibrosis and ultimately liver cancer (Colombo and Lleo 2018). Furthermore, alcohol consumption increases the risk of liver cancer, with long-term heavy drinking

potentially causing liver damage and liver cancer occurrence (He et al. 2021).

Despite significant advancements in the diagnosis and treatment of liver cancer, there are still some issues to be solved. Specifically, liver cancer is a malignant tumor with a high degree of malignancy, easy metastasis and rapid relapse, thus leading to poor treatment outcomes (Anwanwan et al. 2020). Traditional treatment modalities for liver cancer, including chemotherapy and radiotherapy, not only have severe cytotoxic effects on tumor cells but also cause accompanying damage to normal cells or organs (Gao et al. 2019). Moreover, massive genomic variation in liver cancer easily causes tumor cells to develop resistance to chemotherapy drugs, leading to treatment failure (Nia and Dhanasekaran 2020). As expected, more precise cancer treatments, such as immunotherapy and gene therapy, might be employed to improve therapeutic efficacy (Rangel-Sosa et al. 2017), or even genomic- and proteomic-based techniques could be used for further investigations of the mechanism of liver cancer resistance to develop effective therapeutic approaches (Cao et al. 2019). However, some prevention interventions, such as improving diet and nutrition, are also important strategies for preventing the occurrence of liver cancer.

Edible oil, an essential ingredient for our daily diet, contains a variety of fatty acids (FAs), such as saturated FAs and mono- and polyunsaturated FAs. According to carbon chain length, FAs are divided into short-chain fatty acids (≤ 6 carbon atoms), medium-chain fatty acids (7-12 carbon atoms) and long-chain fatty acids (≥ 12 carbon atoms) (Fauser et al. 2011). Fatty acids are important components of the body and have many significant biological functions (de Carvalho and Caramujo 2018; Stamenkovic et al. 2019). For instance, medium-chain fatty acids (MCFAs), such as octanoic acid, decanoic acid and dodecanoic acid (DDA), which are abundant in coconut oil, palm oil and milk, are involved in the construction of cell membranes, serve as energy sources, or even function as cell signals (Devi and Khatkar 2018; Panth et al. 2018). Publications have reported the effects of MCFA on health and diseases, such as improving metabolic diseases and suppressing fat accumulation. In the study of Kono and his coworkers (2003), medium chain triglyceride (MCT) was found to prevent LPS-mediated endotoxemia, which is associated with obesity and metabolic syndrome. St-Onge et al. (2008) reported that MCT was involved in weight loss without adversely affecting normal metabolic activity. As one of the important MCFA representatives, DDA comprises approximately 50% of the fatty acids in coconut oil and has many applications (Sankararaman and Sferra 2018). Liu et al. (2018) fed 1-day-old chickens dietary supplement containing DDA and observed that it effectively improved the growth performance and digestive capacity of chickens. Additionally, evidence has demonstrated that DDA and its derivatives have strong antibacterial activity against gram-positive bacteria by destroying the bacterial membrane (Bergsson et al. 2001). Additionally, DDA has been reported to improve cardiovascular health status because of its ability to increase high-density lipoprotein levels and decrease blood pressure (Eyres et al. 2016).

Moreover, studies have reported the anticancer potential of DDA against some tumor types. In the study of Veeresh Babu and his coworkers (2010), a certain dosage of DDA was observed to prevent testosterone-induced prostatic hyperplasia in rats. Similarly, Jiao et al. (2008) reported that the growth of ovarian cancer cells cultured in DDA-containing media was significantly greater than that of control cells. This kind of MCFA also exerted anti-proliferative and pro-apoptotic effects on breast and endometrial cancer cells (Lappano et al. 2017), fully illustrating the anticancer activity of DDA. Notably, as reported by Conceição et al. (2016), DDA could obviously prolong survival and improve quality of life in breast cancer patients during chemotherapy treatment. In addition, DDA has been shown to have antineoplastic and proapoptotic effects on intestinal cancer cells (Fauser et al. 2013). Compared with long-chain fatty acids, MCFAs, including DDA, can more significantly alleviate the fatigue of terminal cancer patients (Narayanan et al. 2015; Mori et al. 2019). Based on the above review, the present research mainly focused on the role of DDA in reproductive cancers (ovarian cancer, prostate cancer, and endometrial cancer) and colon cancer, whereas very few studies have focused on the effect of DDA on liver cancer. Therefore, this study treated Hepa 1-6 liver cancer cells with DDA and evaluated the impact of this fatty acid on liver cancer by detecting cell viability, cell cycle progression, cell apoptosis, intercellular redox status and mitochondrial function. This study sheds light on the possible mechanism by which DDA regulates the growth of liver cancer cells to a certain extent.

2. Material and Methods

Materials

Hepa 1-6 cell lines and Dulbecco's modified Eagle's medium (DMEM) were purchased from Procell Life Science & Technology Co., Ltd. (Wuhan, China). DDA was obtained from Macklin Biochemical Co., Ltd. (Shanghai, China). Fetal bovine serum (FBS) and fatty acid-free (FAF)-bovine serum albumin (BSA) were obtained from CellMax Co., Ltd. (Beijing, China). CCK8 was purchased from Biosharp (Hefei, China). Assay kits for SOD, GSH, ROS, ATP and mitochondrial membrane potential (JC-1) were obtained from Nanjing Jiancheng Bioengineering Institute (Nanjing, China). A BCA protein assay kit, an Annexin V-FITC/PI apoptosis detection kit and a DNA assay kit were obtained from Solarbio Co., Ltd. (Beijing, China). A Hoechst 33258 staining kit was obtained from Beyotime Institute of Biotechnology (Shanghai, China). Primary antibodies against Caspase 3, Bcl-2 and Bax were obtained from Bioworld (Wuhan, China). The secondary antibodies (goat anti-rabbit and goat anti-mouse) were obtained from Bioworld and EpiZyme (Shanghai, China), respectively.

Cell culturing

Hepa 1-6 cells were first cultured in DMEM supplemented with 10% FBS after the cells were defrosted. When they reached 70-80% confluence, the cells were digested with 0.25% trypsin and subcultured. The passaged cells were then seeded in a cell culture plate for DDA treatment or in a cell flask for passage under a humidified atmosphere at 37 °C in 5% CO₂. Note: All experiments were performed in accordance with the relevant approved guidelines and regulations, as well as under the approval of the Medical Ethics Committee of the First Affiliated Hospital of Henan University of Science and Technology.

Grouping and DDA treatment

Hepa 1-6 cells in the logarithmic growth phase were trypsinized, harvested and seeded into a 96-well plate at a concentration of 2×10^5 cells/mL in 100 μ L (each well) DMEM supplemented with 10% FBS (fetal bovine serum). After 24 h of incubation, the culture medium was replaced with 100 μ L of complete DMEM containing freshly prepared DDA (1 mol/L), which was conjugated to 0.4% FAF-BSA at final concentrations of 0.1, 0.3, 0.5, 1, 2 and 4 mM, and then incubated for 24 h, 48 h or 72 h to determine the optimal DDA concentration via the CCK-8 assay. Untreated DDA-treated cells were used as a control.

CCK-8 assay

CCK-8 (Cell Counting Kit-8) is widely used for determining cell viability via cell proliferation and cytotoxicity assays on the basis of WST-8, an MTT-like compound that is reduced to yellow formazan dye by dehydrogenases in viable cells (Cai et al. 2019). The amount of formazan dye produced is directly proportional to the number of viable cells. Briefly, after treatment with various concentrations of DDA for 24 h, 48 h and 72 h, the cells were harvested as described above and washed twice in PBS, after which 100 μ L of 0.4% FAF-BSA-supplemented DMEM and 10 μ L of CCK-8 solution were added to each well. After 2 h of incubation, a microplate reader was used to measure the absorbance at 450 nm.

Hoechst 33258 staining

Hepa 1-6 cells were plated in 6-well plates (1×10^5 cells/well) and cultured for approximately 12-16 hours. After treatment with 0.5 mM DDA for different durations (24 h, 48 h, 72 h), the cells were fixed with 4% formaldehyde for 10 min and then manually washed twice with PBS. The cells were stained with 0.5 mL of Hoechst 33258 (Beyotime, Shanghai, China) for 5 min at room temperature, followed by washing three times in PBS. Finally, the cells were observed and photographed under a fluorescence microscope (Zeiss, Germany; excitation/emission wavelengths: 350/460 nm; magnification: $\times 200$).

Cell cycle analysis

The cells were seeded in a 6-well plate at a concentration of 2×10^5 cells/mL and routinely cultured overnight. After washing twice with DMEM containing 0.4% FAF-BSA, the cells were incubated in medium containing the optimal concentration of DDA for 24 h, 48 h or 72 h. The cells from each group were digested, harvested and fixed in precooled 70% ethanol overnight and then treated with RNase A solution at 37 °C for 30 min, followed by PI staining for 30 min at 4 °C in the dark using a DNA content quantitation assay kit (Solarbio, Beijing). The cell cycle distribution was analyzed by flow cytometry (Beckman, USA) via FACS analysis. At least three independent experiments were carried out.

Apoptosis detection

Cell culture, grouping and DDA treatment were performed as previously described. Cell apoptosis was assessed by Annexin V-FITC/PI staining based on the instructions of the Annexin V-FITC apoptosis detection kit (Solarbio, Beijing). Briefly, the harvested cells were washed twice in precooled PBS. The cells were resuspended at a density of 1×10^6 cells/mL in $1 \times$ binding buffer, and 100 μ L of the cell suspension ($\sim 1 \times 10^5$ cells) was collected and then incubated with Annexin V-FITC (5 μ L) for 10 min and PI (5 μ L) for 5 min in the dark at room temperature. Then, 500 μ L of PBS buffer was added to reach a final concentration of $\sim 0.15 \times 10^6$ cells/mL. Finally, flow cytometry (Beckman, USA) was used to analyze the cell apoptosis rate. Three independent experiments were performed.

Western blot analysis

Immunoblot analysis was performed to assess the expression of the apoptosis-related proteins Bcl-2, Bax and Caspase-3. Hepa 1-6 cells were treated with the optimal DDA concentration for 24 h, 48 h or 72 h. The cells were harvested and lysed in ice-cold RIPA buffer supplemented with protease inhibitor (EpiZyme, Shanghai, China) for 30 min and centrifuged at 12000 rpm for 5 min at 4 °C. The supernatant containing total proteins was collected and quantified by a BCA protein assay kit (Solarbio, Beijing, China). Equal amounts of denatured protein extracted from untreated or DDA-treated cells were loaded onto a 12.5% SDS-PAGE gel and transferred to a PVDF membrane. Protein blocking was performed with 5% skim milk in TBS Tris-buffered saline supplemented with 0.1% Tween-20 (TBST) for 2 hours. After washing three times with TBST, the membranes were probed with specific primary antibodies, including a Bcl-2 rabbit polyclonal antibody (pAb, 1:1000), a Bax rabbit pAb (1:1000), and a caspase-3 rabbit pAb (1:1000), in 5 ml of blocking buffer overnight at 4 °C. β -Actin (1:8000) served as an internal control. Next, the membranes were washed three times with TBST and incubated with the appropriate secondary antibodies for 1 h at room temperature. Finally, the membranes were incubated with an ECL solution and then imaged on an Amersham Imager 600 (GE, USA) followed by quantification using ImageJ software.

Determination of oxidative stress indices

After treatment with the indicated concentrations of DDA for 24 h, 48 h or 72 h, the cells were collected, and the levels of oxidative stress markers were measured.

SOD activity was assayed as follows: after the harvested cells were centrifuged at 1000 rpm for 20 min, the supernatant was discarded. The pellet was resuspended at 3×10^6 cells/mL in PBS, followed by cell disruption through sonication. After centrifugation, the supernatant was collected and diluted 10 times with PBS. A 20 μ L sample was added to each well of a 96-well plate to detect SOD activity. SOD activity was determined using SOD assay kits (Nanjing Jiancheng Bioengineering Institute, China) and is expressed as units per microgram of total protein (U/mg). The total protein concentration was quantified using a bicinchoninic acid (BCA) protein assay kit (Solarbio, Beijing, China).

Intracellular reactive oxygen species (ROS) levels were measured using an ROS assay kit (Nanjing Jiancheng Bioengineering Institute, China). The cells were trypsinized, collected and centrifuged at 1000 rpm for 10 min and then resuspended in PBS. The cell suspensions were incubated with a final concentration of

10 μM DCFH-DA reagent at 37 °C for 1 h and centrifuged at 1000 rpm for 5 min. The dissociated pellets were resuspended in PBS to a final concentration of 1×10^6 cells/mL, 200 μL of sample was added to a 96-well opaque white plate (Jing'an Hi-Tech, Jiangxi, China), and the fluorescence intensity of DCF was measured (Ex at 500 nm; Em at 525 nm) using a Spark multimode microplate reader (Tecan, Männedorf, Switzerland). The intensity of fluorescence was proportional to the ROS concentration.

The intracellular GSH content was determined by a GSH assay kit (Nanjing Jiancheng Bioengineering Institute, China) following the manufacturer's guidelines. Cell harvesting was performed as described above. After centrifugation, the precipitated cells were resuspended to a concentration of 1×10^6 cells/mL. After the cells were crushed with an electric grinder, the supernatant was collected to determine the GSH content. Then, 100 μL of buffer solution and 25 μL of chromogenic reagent were added to 100 μL of cell supernatant and sufficiently mixed. Finally, the reaction was monitored at 405 nm under a microplate reader (Tecan Spark, Männedorf, Switzerland). Total protein concentrations were determined by using a BCA protein assay kit. The GSH content was expressed as $\mu\text{mol/gprot}$.

Mitochondrial membrane potential (MMP) assay

The MMP was determined using an MMP assay kit (Nanjing Jiancheng Bioengineering Institute, China). Specifically, Hepa1-6 cells were exposed to the indicated DDA concentrations for 24 h, 48 h or 72 h, washed in precooled PBS and then harvested. The collected cells were resuspended in JC-1 working solution (diluted 1:500) to a final density of 2×10^6 cells/mL, incubated for 20 min at 37 °C, and centrifuged at 2000 rpm for 5 min at room temperature. The supernatant was discarded, and the pellets were washed and resuspended in $1 \times$ incubation buffer for subsequent flow cytometric analysis with a CytoFLEX Flow Cytometer (Beckman Coulter). Normal mitochondria containing red JC-1 aggregates were detected by PI, and apoptotic cells containing green JC-1 monomers were detected by FITC.

Cellular ATP level determination

After treatment with the optimum concentration of DDA for different durations at 37 °C, as mentioned above, the cells (approximately 1×10^6) were harvested, heated for 10 min in a boiling water bath and centrifuged at 4000 rpm for 5 min. The precipitate was removed, 30 μL of supernatant was added to each well, and a 96-well microplate was placed in a microplate reader (Tecan Spark, Männedorf, Switzerland) for measuring the mitochondrial ATP level at 636 nm according to the protocol of the ATP content assay kit (Nanjing Jiancheng Bioengineering Institute, China). The total protein concentration was determined by the BCA method. The cellular ATP level was expressed as $\mu\text{mol/gprot}$.

Statistical analysis

The data are expressed as the mean \pm standard deviation (SD), and all experiments were independently repeated three times. The data analysis was performed using SPSS 17.0 software. Differences among experimental groups were analyzed by one-way ANOVA followed by Dunnett's test. A P value < 0.05 was considered to indicate a statistically significant difference.

3. Results

DDA inhibits the viability of liver cancer cells

After Hepa1-6 liver cancer cells were treated with different concentrations of DDA (0.1, 0.3, 0.5, 1, 2 and 4 mM) for 24 h, 48 h and 72 h, a CCK-8 assay was used to assess cell viability. As illustrated in Figure 1, DDA at concentrations less than 0.5 mM (0.1 or 0.3 mM) did not obviously impact the viability of the Hepa 1-6 cells (those above 70%). For instance, the cell survival rate reached 76.51% at 72 h after treatment with 0.1 mM DDA but reached approximately 80% at 24 h after treatment with 0.3 mM DDA. At concentrations greater than 0.5 mM (1, 2, or 4 mM), DDA significantly inhibited the growth of Hepa1-6 cells and decreased

cell viability in a dose- and time-dependent manner ($P < 0.05$). Briefly, the cell survival rate decreased to 12.87% after treatment with 1 mM DDA for 48 h and decreased to only 7.56% after treatment with 4 mM DDA for 24 h. Despite having lower cell viability than the control, a DDA concentration < 0.5 mM had a relatively weak effect on inhibiting liver tumor cell growth, whereas a high concentration (> 0.5 mM) of DDA had strong toxicity to the cells. Therefore, 0.5 mM DDA was considered the optimal concentration for subsequent experiments.

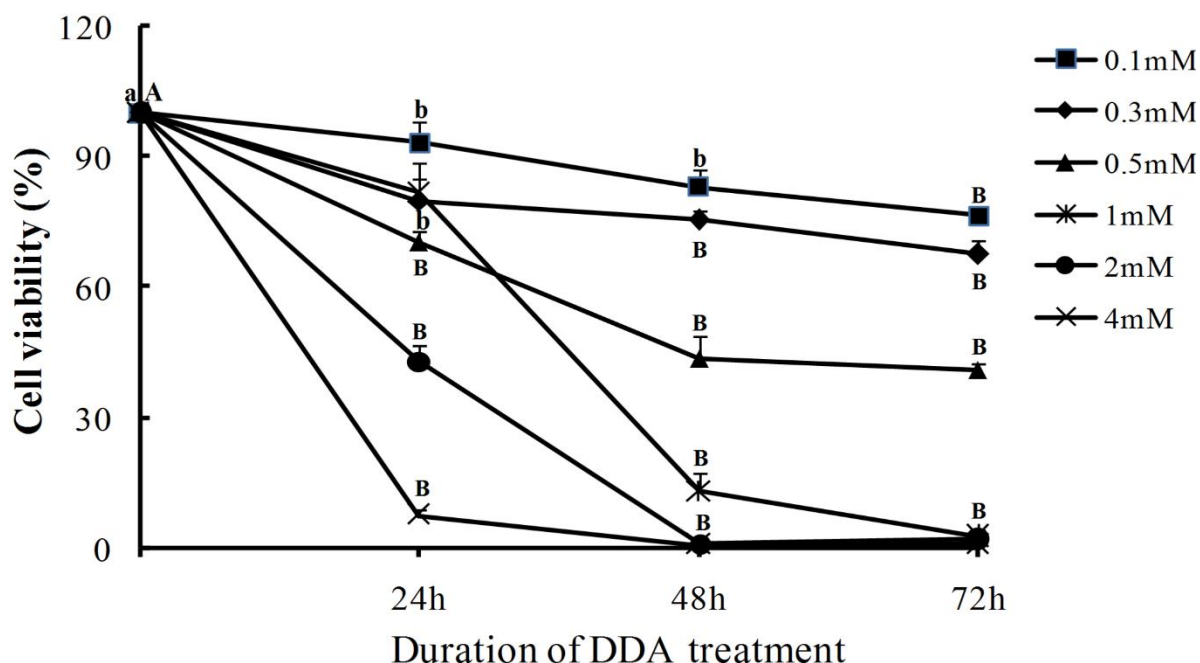


Figure 1. The effect of different concentrations of DDA on the survival rate (%) of Hepa 1-6 cells after different durations of treatment. The capital letter B indicates an extremely significant difference ($P < 0.01$) compared with 0 h (control); the lower letter b indicates a significant difference ($P < 0.05$) compared with 0 h (control).

To further explore the effect of DDA on cell morphology, morphological changes in Hepa 1-6 cells after treatment with 0.5 mM DDA were observed under an inverted microscope. As shown in Figure 2, the cells in the control group were in good condition with a uniform cell distribution, adherent growth and clear cell outline, while the DDA-treated cells showed severe changes in morphology characterized by an unfixed size, unclear outline, cell death (e.g., the appearance of floating cells and cell debris) and growth inhibition (e.g., an obvious decrease in cell density). The longer the treatment duration was, the more severe the cell morphological alterations were.

DDA might block cell division in Hepa 1-6 cells

The cell cycle distribution of Hepa1-6 cells treated with 0.5 mM DDA was analyzed by flow cytometry, and the results are shown in Figure 3A (left panel). Compared to that of the untreated control (62.0%), the proportion of cells in the G1 phase decreased to 61.0% at 24 h ($P > 0.05$), decreased to 62.05% at 48 h ($P > 0.05$), and then decreased to 53.47% at 72 h ($P < 0.01$). For S phase, there was an extremely significant difference between the DDA-treated group and the control group ($P < 0.01$), and the percentage of Hepa 1-6 cells in S phase increased in a time-dependent manner after DDA treatment (12.56% at 24 h, 19.5% at 48 h and 22.98% at 72 h; $P < 0.01$) compared to that in the control group (6.99%). For the G2/M phase, DDA-treated groups were also highly significantly different from the control group ($P < 0.01$), and the population of cells greatly decreased from 28.32% in the control group to 21.80% at 24 h, 13.86% at 48 h, and 7.73% at 72 h ($P < 0.01$) in a time-dependent manner.

In addition, compared with that in the control group (3.14%), the sub-G1 population, which indicates apoptosis-associated chromatin degradation, significantly increased in the DDA-treated group and even

peaked at 72 h (34.50%, $P < 0.01$; Figure 3B). Based on the above results, DDA treatment leads to cell cycle arrest in the S phase, as evidenced by the increasing proportion of S-phase cells but the decreasing proportion of cells in both the G1 and G2/M phases.

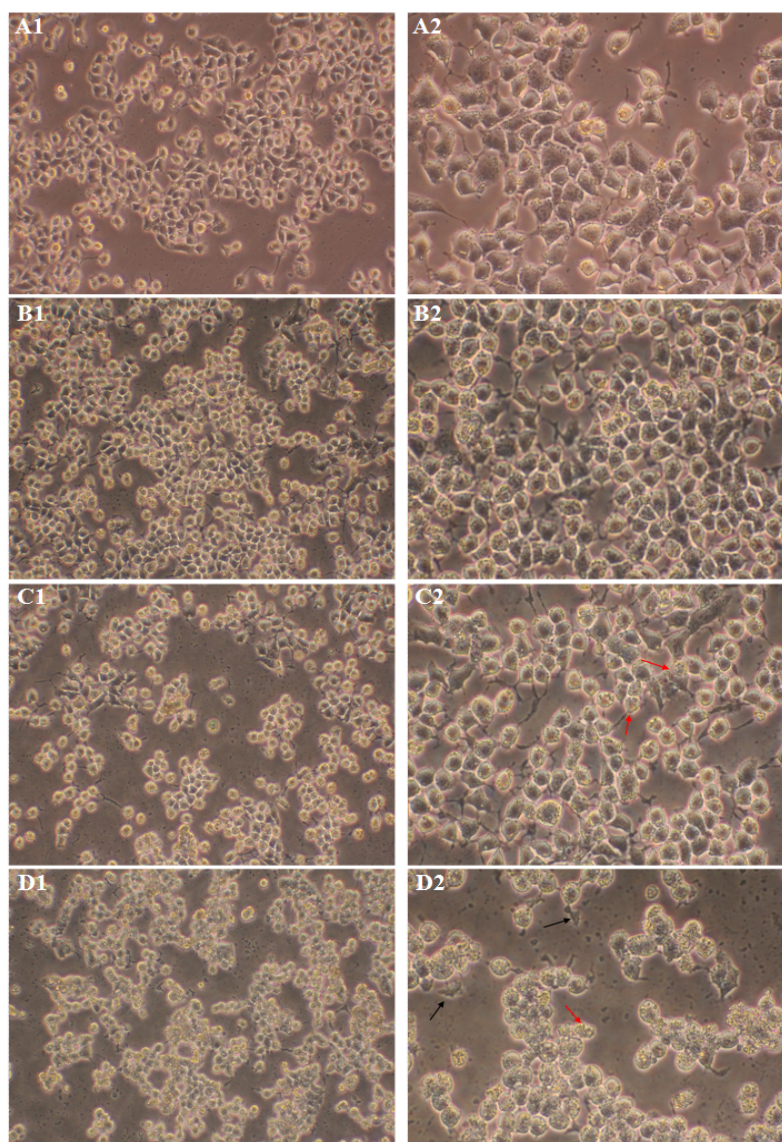


Figure 2. The cells were observed under an inverted microscope after treatment with 0.5 mM DDA for the indicated times. A – Control group; B – DDA-treated 24 h group; C – DDA-treated 48 h group; D–DDA-treated 72 h group. Red arrows: cells of unfixed size with unclear outlines; black arrows: cell debris. Left column: magnification $\times 100$; Left column: magnification $\times 200$

DDA induces apoptotic death in Hepa1-6 cells

After different durations of treatment with 0.5 mM DDA, the Hepa1-6 cells were stained with Hoechst 33258 and observed under a fluorescence microscope (200 \times). As shown in Figure 4, blue-stained nuclei were dyed with Hoechst 33258, a blue fluorescence dye that stains condensed chromatin in apoptotic cells more brightly than chromatin in normal cells. Morphological apoptotic changes, such as condensed nuclei and nuclear fragmentation, were observed in the DDA-treated groups (Figure 4B–D), while few apoptotic cells were observed in the control group (Figure 4A).

Furthermore, flow cytometric analysis of Annexin V-FITC/PI double-staining was performed to estimate the cell apoptotic rate. As shown in Figure 5, there was a time-dependent increase ($P < 0.01$) in the total cell apoptotic rate after treatment with DDA compared to that in the control group. Briefly, the percentage of early apoptotic cells after 24 h of DDA treatment (3.53%) did not significantly ($P > 0.05$) differ

from that of the control (2.86%); the percentage of early apoptotic cells significantly ($P<0.01$) increased to 17.37% at 48 h and to 21.70% at 72 h in comparison with that of the control (Figure 5B). Similarly, the percentage of late apoptotic/necrotic cells in the DDA-treated groups (11.07% at 48 h, 13.57% at 72 h) was also significantly greater than that in the control group (1.60%, $P<0.01$); at 24 h after treatment with DDA, the percentage of late apoptotic cells did not differ from that in the control group ($P>0.05$).

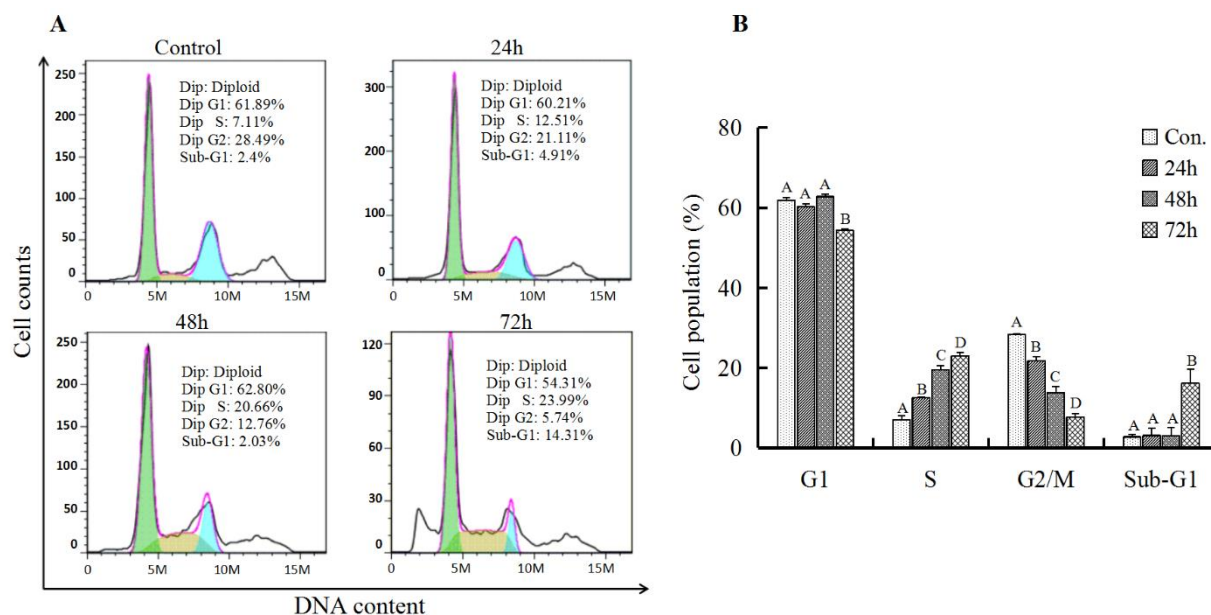


Figure 3. Flow cytometric analysis of the cell cycle distribution of Hepa 1-6 cells after treatment with 0.5 mM DDA. DDA inhibits the progression of cell division by arresting cells in the S phase. A – Representative flow cytometry histograms showing the DNA content of Hepa 1-6 cells treated with 0.5 mM DDA for 24 h, 48 h and 72 h. B – Analysis of the cell cycle distribution in each group (n=3). Cells were treated for different durations and then subjected to PI staining. DNA content was measured by flow cytometry. Analysis was performed using SPSS 17.0 software with an ANOVA statistical model. The data are presented as the percentage of cells in the sub-G1, G1, S and G2/M phases. For each sample, 1×10^6 cells were acquired. The data shown are the means \pm SDs. Comparisons between different experimental groups using Dunnett's multiple comparison tests are shown in the figure. Different superscript capital letters indicate extremely significant differences ($P<0.01$); the same superscript letters indicate no significant difference (n=3, $P>0.05$).

DDA induced oxidative stress in hepatic cancer cells

This study assayed biomarkers of oxidative stress, including cellular ROS production, GSH content and SOD activity, in Hepa 1-6 cells treated with 0.5 mM DDA for different durations. As shown in Figure 6A, after treatment with DDA, ROS production in the cells significantly increased in a time-dependent manner ($P<0.01$); moreover, the GSH content clearly decreased compared to that in the control group (Figure 6B, $P<0.01$). The activity of total SOD (T-SOD), an important endogenous antioxidative enzyme, was determined by a SOD assay kit. As shown in Figure 6C, compared to that in the control group (12.01 U/mg prot), the T-SOD activity in the DDA-treated groups gradually decreased with increasing treatment time, which was opposite to the trends in the ROS and GSH levels. Statistical analysis revealed a significant difference in T-SOD activity only at 72 h of treatment (9.23 U/mgprot) compared with that of the control (12.01 U/mgprot, $P<0.01$).

DDA impacts the mitochondrial membrane potential of Hepa 1-6 cells

The MMP is a key parameter indicating mitochondrial function, and a decrease or increase in the MMP could impact cell viability. In this study, MMP alterations in cells treated with 0.5 mM DDA for different durations were measured by a JC-1 assay kit using flow cytometry. As displayed in Figure 7, the cells in the

control group had a relatively high MMP, which was indicated by the high percentage of viable cells (79.13%). Compared with that in the control group, the MMP was lower in the DDA-treated group, implying that JC-1 accumulated less in the mitochondrial matrix for J-aggregate formation (Figure 7A). Furthermore, the MMP could be effectively decreased ($P<0.01$) by 0.5 mM DDA in a time-dependent manner (Figure 7B).

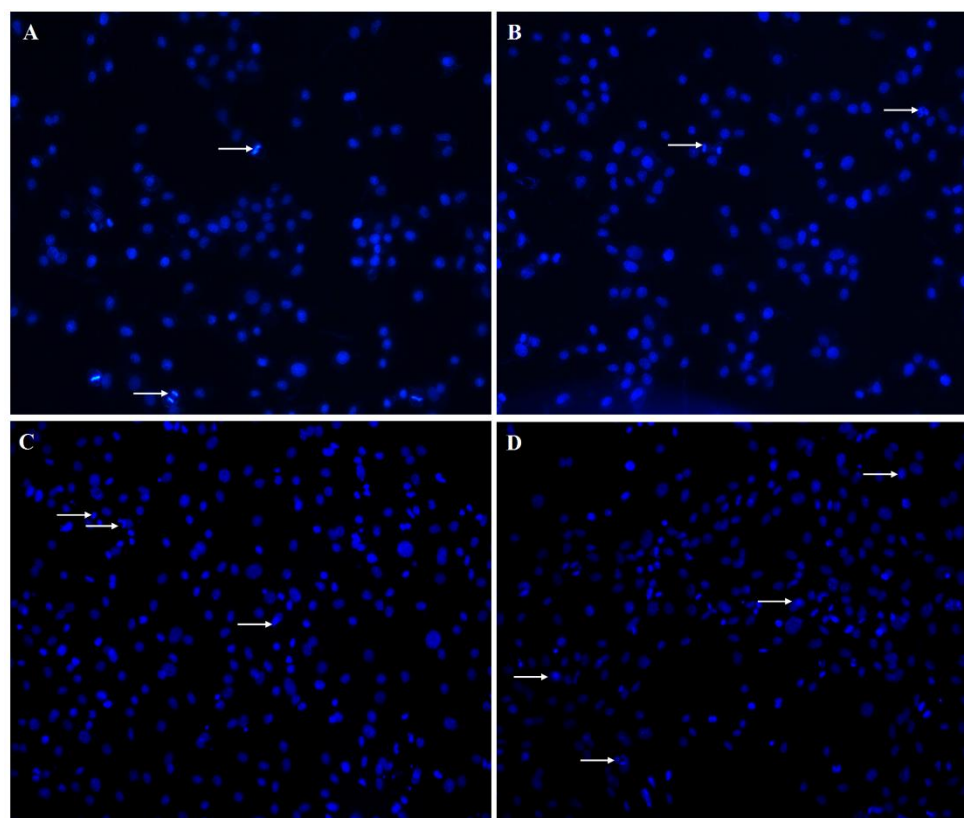


Figure 4. Photograph showing the results of Hoechst 33258 staining of Hepa 1-6 cells (200 \times). After the cells were treated with 0.5 mM DDA for the indicated times, the apoptotic cells were observed by Hoechst 33258 staining under a fluorescence microscope. A – control group; B – 0.5 mM DDA treatment for 24 h; C – 0.5 mM DDA treatment for 48 h; D – 0.5 mM DDA treatment for 72 h. The apoptotic cells are indicated by arrows.

DDA reduces ATP levels in Hepa 1-6 cells

In eukaryotes, mitochondria are the main site of ATP synthesis. A decrease in ATP levels implies a decrease or even loss of mitochondrial function, and a reduction in ATP levels during apoptosis usually coincides with a decrease in the MMP. For this reason, our study evaluated the effect of DDA on ATP production in Hepa 1-6 cells using an ATP determination kit. Compared with that in the control group (939.31 $\mu\text{mol/gprot}$), the level of cellular ATP decreased in a time-dependent manner with treatment time (877.15 $\mu\text{mol/gprot}$ at 24 h; 790.55 $\mu\text{mol/gprot}$ at 48 h; 513.81 $\mu\text{mol/gprot}$ at 72 h), as shown in Table 1. According to the statistical analysis, the ATP content significantly differed ($P<0.05$) after 24 h of treatment and significantly differed after 48 h and 72 h ($P<0.01$) compared with that of the control.

Table 1. Changes in ATP levels in cells after administration of 0.5 mM DDA for different durations.

Grouping	ATP level ($\mu\text{mol/gprot}$)
Control	939.31 \pm 18.25 ^{Aa}
24h treatment	877.15 \pm 23.99 ^{Ab}
48h treatment	790.55 \pm 29.85 ^{Ba}
72h treatment	513.81 \pm 34.15 ^{Ca}

Note: Within the same column, different superscript lowercase letters and capital letters indicate significant differences ($P<0.05$) and very significant differences ($P<0.01$), respectively; the same superscript letters represent no significant difference ($P >0.05$).

DDA modulates the expression of apoptosis-related proteins

To further investigate whether DDA-mediated cell apoptosis was related to intrinsic mitochondrial activity, the protein expression of Bcl-2, Bax and Caspase-3 was measured by western blotting after incubation with 0.5 mM DDA for 24 h, 48 h and 72 h. As shown in Figure 8, 0.5 mM DDA significantly upregulated the expression of the pro-apoptotic protein Bax and downregulated the expression of the anti-apoptotic protein Bcl-2 and the ratio of Bcl-2 to Bax in a time-dependent manner ($P < 0.01$); clearly, a decrease in the Bcl-2 protein level was associated with an increase in Bax. Similar to that of Bax, the protein expression of Caspase-3 was significantly upregulated in the cells treated with DDA ($P < 0.01$).

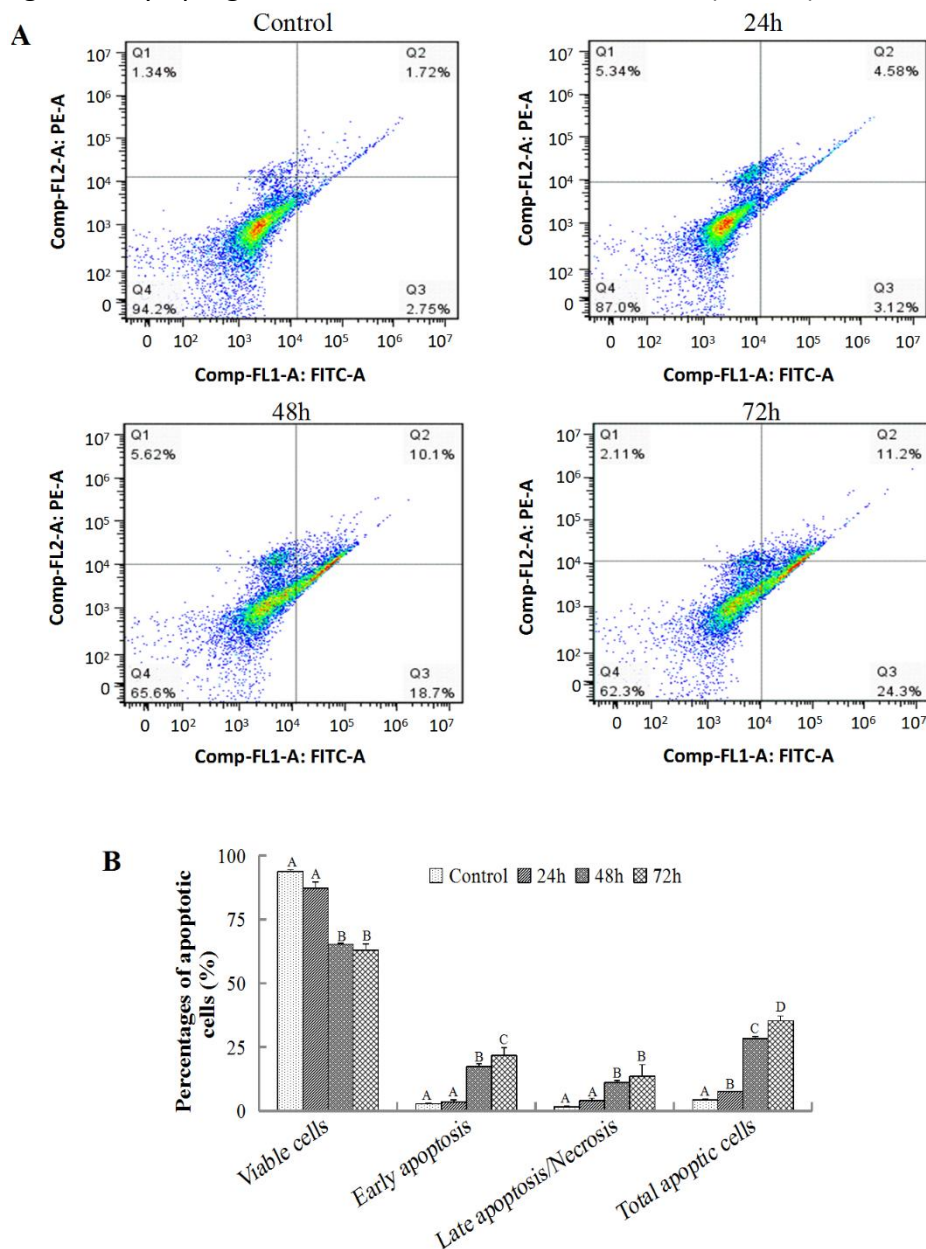


Figure 5. Apoptosis analysis of Hepa 1-6 cells treated with DDA for the indicated times. A – Representative dot plots showing the results of flow cytometric analysis of Hepa 1-6 cells. The cells were treated with 0.5 mM DDA for the indicated time periods (24 h, 48 h and 72 h) and then stained with Annexin V-FITC/PI; B – Schematic diagram showing the evaluation of the apoptotic index in each group (n=3). The data shown are the means \pm SDs. Comparisons between different groups using Dunnett's multiple comparison tests are shown in the figure. Different superscript capital letters indicate extremely significant differences ($P < 0.01$); the same superscript letter indicates no significant difference ($P > 0.05$).

4. Discussion

As a kind of medium-chain saturated fatty acid, DDA is an important component of many vegetable oils, especially coconut oil and palm kernel oil (Schwab et al. 1995). At present, this fatty acid has been extensively used in many fields, including food, medicine and daily chemicals (Zeiger et al. 2017; Santos et al. 2019). With increasing DDA application, it has been found that DDA can markedly inhibit the growth of some tumor burdens in the prostate, breast, stomach and lung (Silva et al. 2018; Sheela et al. 2019; De Matteis et al. 2019). However, it remains unclear whether this fatty acid exerts an antitumor effect on liver cancer.

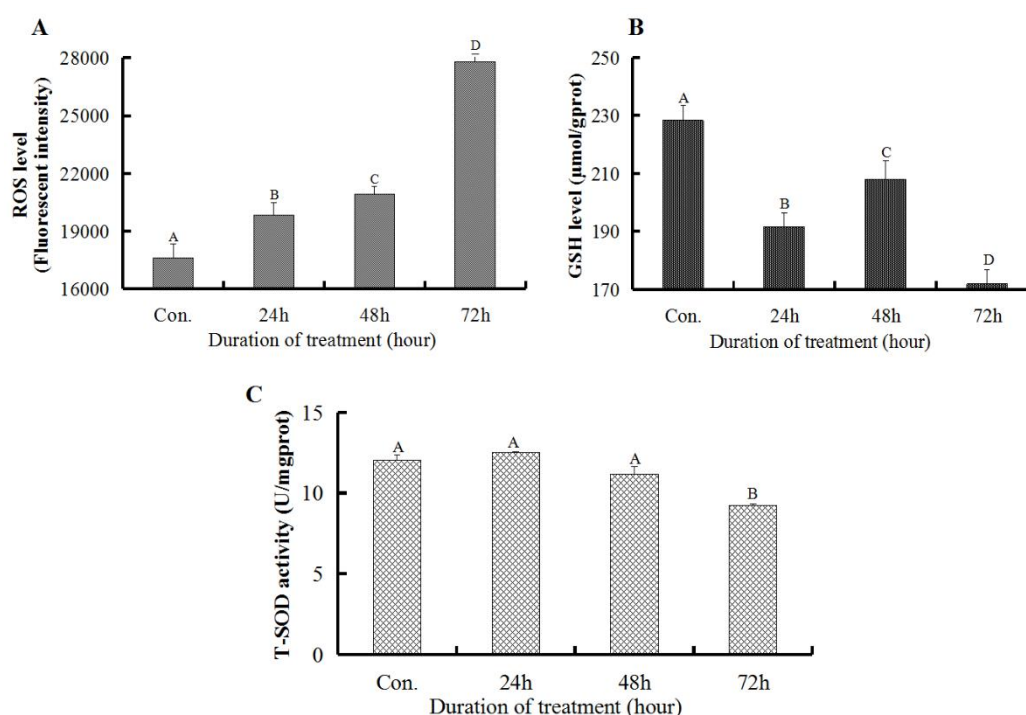


Figure 6. Oxidative stress markers in Hepa1-6 cells treated with 0.5 mM DDA. The effect of 0.5 mM DDA on biomarkers of oxidative stress and antioxidant status. A – reactive oxygen species (ROS) level; B – glutathione (GSH) content; C – total superoxide dismutase (T-SOD) activity. The values are shown as the means \pm SDs. Bars with the same capital letter are not significantly different ($P > 0.05$); bars with different capital letters are significantly different ($P < 0.01$). Significant differences among groups were analyzed using one-way ANOVA with Dunnett's multiple comparisons test ($P < 0.05$, $n=3$).

In this study, Hepa 1-6 liver cancer cells were used as experimental subjects and treated with different concentrations of DDA ranging from 0.1 mM to 4.0 mM for different durations. As a result, all concentrations of DDA had varying degrees of inhibitory effects on cell viability. However, the effect of $DDA < 0.5$ mM on cell viability was relatively weak, while $DDA > 0.5$ mM was extremely cytotoxic to cultured Hepa 1-6 cells. For this reason, 0.5 mM DDA was identified as the optimal concentration for studying its anti-liver cancer effect and the underlying mechanism.

It has been shown that dodecanoic acid can greatly increase oxidative stress in colon cancer cells in vitro (Fauser et al. 2013). Accordingly, it could be hypothesized that DDA-induced oxidative stress causes cell division cycle arrest and apoptosis. In this study, the induction of oxidative stress in liver cancer cells was reflected by an increase in intercellular ROS levels, a decrease in GSH and a decrease in SOD activity, which was consistent with the results of Fauser et al., who reported that DDA increased cellular ROS levels but decreased GSH levels. GSH is considered an important nonenzymatic member that controls redox balance in antioxidative systems and can directly scavenge reactive oxygen-derived free radicals (Vigilanza et al. 2011). Especially in cancer cells, high GSH levels are necessary to scavenge excessive ROS. Taken together, as shown in Figure 9, the increase in ROS observed in this study was possibly related to the failure to

scavenge excessive ROS in DDA-treated cells in a timely manner due to the depletion of GSH. Enzymatic antioxidants, including SOD, are responsible for the removal of various ROS (i.e., superoxide anion radicals, hydrogen peroxide, etc.), thus maintaining the intracellular redox status (Oka et al. 2015). Our findings showed that DDA significantly reduced the activity of intracellular T-SOD, which might be another cause of the increased ROS level in the cells (Figure 9). Interestingly, the GSH level in all the DDA-treated groups was lower than that in the control group, whereas among the three DDA-treated groups, the GSH level in the cells at 48 h was obviously greater than that at 24 h ($P < 0.01$). Further tests are required to determine the underlying cause.

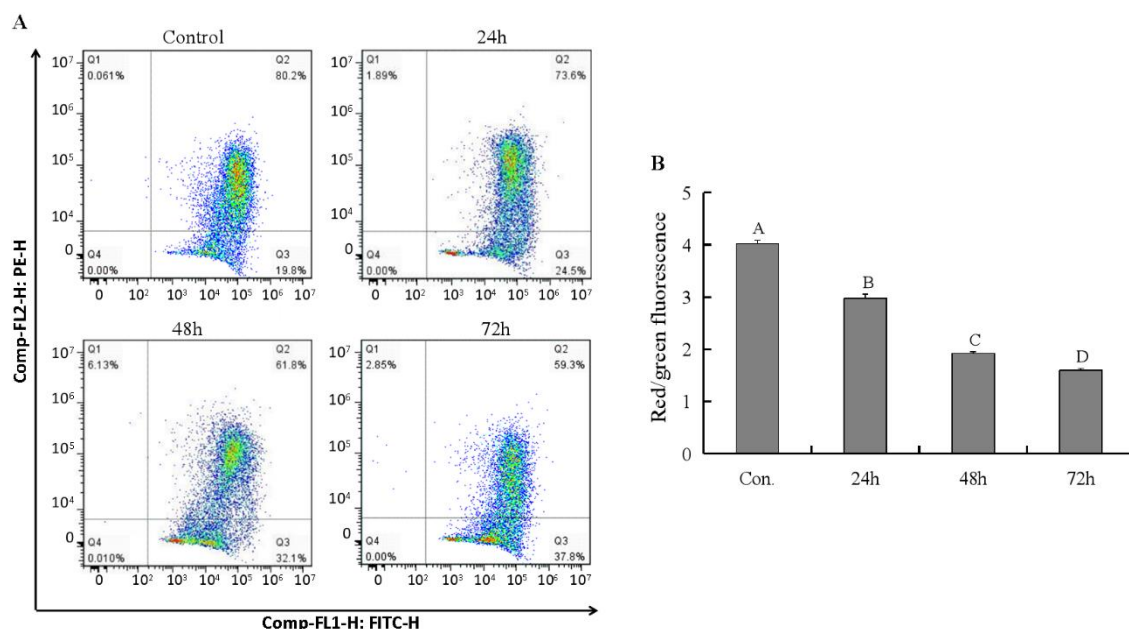


Figure 7. Changes in the mitochondrial membrane potential (MMP) A – Typical MMP patterns of DDA-treated Hepa 1-6 cells treated with 0.5 mM DDA for the indicated times. The MMP was measured by JC-1 fluorescence using flow cytometry. Q1: Necrotic cells, including a small number of late apoptotic cells and mechanically damaged cells; Q2: Late apoptotic cells; Q3: Early apoptotic cells; Q4: Living cells; B – The ratio of red to green fluorescence. The data are expressed as the mean \pm SD. Bars with different capital letters represent statistically significant differences among groups ($P < 0.01$), which were analyzed by one-way ANOVA with Dunnett's test ($P < 0.05$, $n = 3$).

Generally, oxidative stress occurs once ROS production exceeds the antioxidant capacity of the body, which causes cell division arrest or triggers apoptotic cell death (Yang et al. 2018). In this study, the cell cycle distribution and cell apoptosis were further analyzed after treatment with DDA. The percentage of S-phase cells greatly increased, while the percentage of cells in the G1 and G2/M phases severely decreased. The reason may be related to differences in the experimental conditions, experimental procedures or experimental subjects, which need further verification by experiments. These observations obviously differ from a previous report showing that dodecanoic acid reduced the number of colon cancer cells in the G1 phase without affecting S- or G2/M-phase cells (Fauser et al. 2013). Interestingly, DDA significantly induced apoptotic death in Hepa 1-6 cells, as evidenced by flow cytometry analysis and Hoechst staining, which was consistent with reports on the effect of DDA on colon cancer cell apoptosis (Fauser et al. 2013). It could be speculated that DDA preferentially impacts mitosis or cytokinesis rather than DNA replication in liver cancer cells.

Many antitumor substances have been proven to induce apoptotic death in cancer cells via the mitochondrial pathway (Wu et al. 2016; Xiao et al. 2020). Studies have shown that long-chain fatty acids can cause oxidative stress and thus impair mitochondrial function by depolarizing the mitochondrial membrane and opening the permeability transition pore, which thus initiates apoptotic death of the cell (Unger 2002; Rial et al. 2010). However, whether DDA induces cell death through the mitochondrial pathway remains unclear. Mitochondrial-mediated cell death is closely related to the Bcl-2 family (Daniel 2000). Normally, the

proapoptotic protein Bax is located in the cytoplasm and is controlled by the antiapoptotic protein Bcl-2 (Edlich 2018). The presence of an apoptotic stimulus induces Bax translocation to mitochondria, decreases the ratio of Bcl-2/Bax, causes mitochondrial depolarization, triggers the release of cytochrome c and the activation of caspases, and ultimately leads to cell apoptotic death (Kirkin et al. 2004). Accordingly, it could be inferred that the interplay among Bcl-2 family proteins is critical for modulating cell commitment to apoptosis via the mitochondrial pathway. Consistent with a previous report, according to the results of our immunoblot analysis, DDA treatment caused an increase in the Bax protein and a decrease in the Bcl-2 protein in the cells, thus decreasing the ratio of Bcl-2/Bax. In addition, as an important biomarker in the mitochondrial apoptotic pathway, a time-dependent increase in caspase-3 protein levels was also observed in Hepa 1-6 cells after DDA treatment (Figure 9).

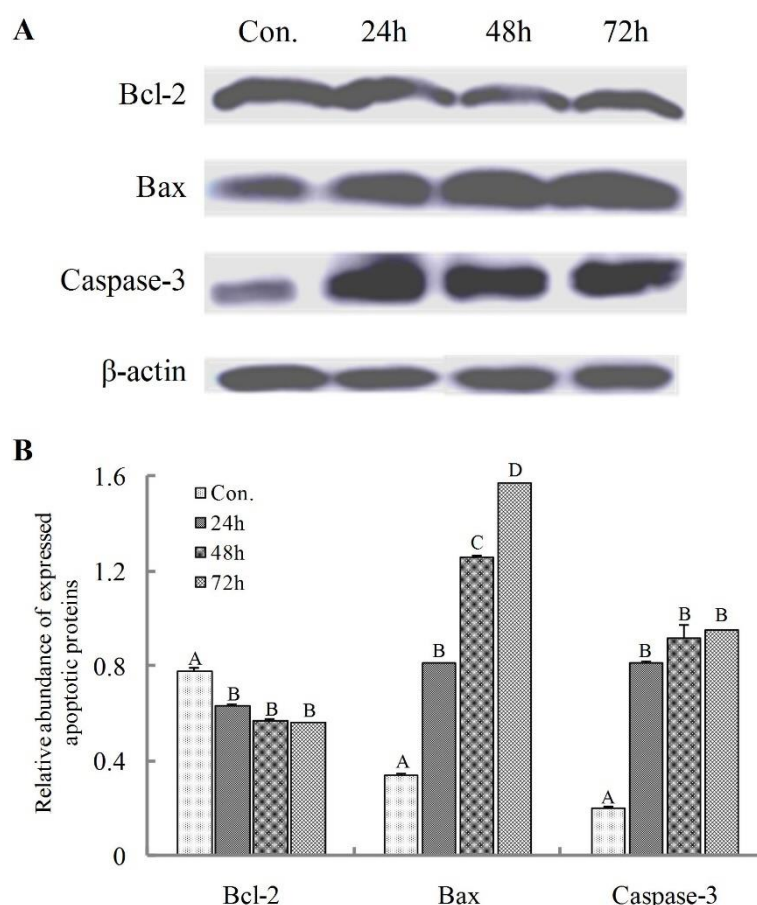


Figure 8. Western blot analysis of the protein expression of Bcl-2, Bax and Caspase 3 in DDA-treated Hepa 1-6 cells. Cells were treated with 0.5 mM DDA for the indicated times. A – Bcl-2, Bax and caspase-3 protein bands. β-Actin served as an internal control. B – Gray-degree value analysis. DDA significantly enhanced Bax and Caspase-3 expression, inhibited Bcl-2 expression, and downregulated the ratio of Bcl-2/Bax in a time-dependent manner. The data are expressed as the means of three independent experiments \pm SD. Columns with different capital letters among the groups differ significantly ($P < 0.01$), and those with the same letters differ insignificantly ($P > 0.05$), as determined by one-way ANOVA with Dunnett's test ($P < 0.05$, $n = 3$). Bcl-2, B-cell lymphoma 2; Bax, Bcl2-associated X protein.

As reported previously, the increased production of ROS first disrupts the mitochondrial membrane potential and consequently causes mitochondrial dysfunction, suggesting the hallmark role of MMP alteration in mitochondrial apoptosis (Palikaras et al. 2015; Angelova and Abramov 2018). Additionally, MMP dissipation has been widely accepted as an indicator of mitochondrial impairment (Galluzzi et al. 2007). In this study, DDA caused mitochondrial dysfunction, as shown by the attenuated MMP and decreased ATP levels in Hepa 1-6 cells treated with DDA. Our data also showed that the change in the MMP was accompanied by a significant decrease in ATP content in parallel. These findings suggested that this medium-chain fatty acid increased the permeabilization of mitochondria, which was correlated with the generation of oxidative stress in the cells.

5. Conclusions

Confronted with the limitations of *in vitro* studies, this study only presented primary evidence of the antitumor activity of DDA and its potential mechanism in liver cancer cells. Based on the above data, a DDA concentration <0.5 mM moderately inhibited the growth of liver tumor cells *in vitro*, whereas a DDA concentration >0.5 mM strongly inhibited the growth and decreased the toxicity of the cells. For this reason, 0.5 mM DDA was selected as the ideal concentration for the mechanism-related studies. It could be concluded that DDA induces oxidative damage in liver cancer cells and leads to mitochondrial dysfunction, thus triggering cell apoptotic death via the mitochondrial pathway. Briefly, DDA perturbs the redox balance in cells, resulting in GSH reduction, excessive ROS generation and decreased SOD activity. A level of oxidative stress beyond the scavenging capacity of the cellular antioxidant system can damage cells, lead to mitochondrial dysfunction, and ultimately trigger mitochondrial apoptotic death (Figure 9).

Despite a preliminary understanding of the role of DDA in liver cancer cells, several questions remain to be answered: how does this fatty acid cause oxidative damage to liver cancer cells, and does DDA disturb cell cycle progression or arrest cytokinesis/nuclear division? These issues need to be solved through in-depth research.

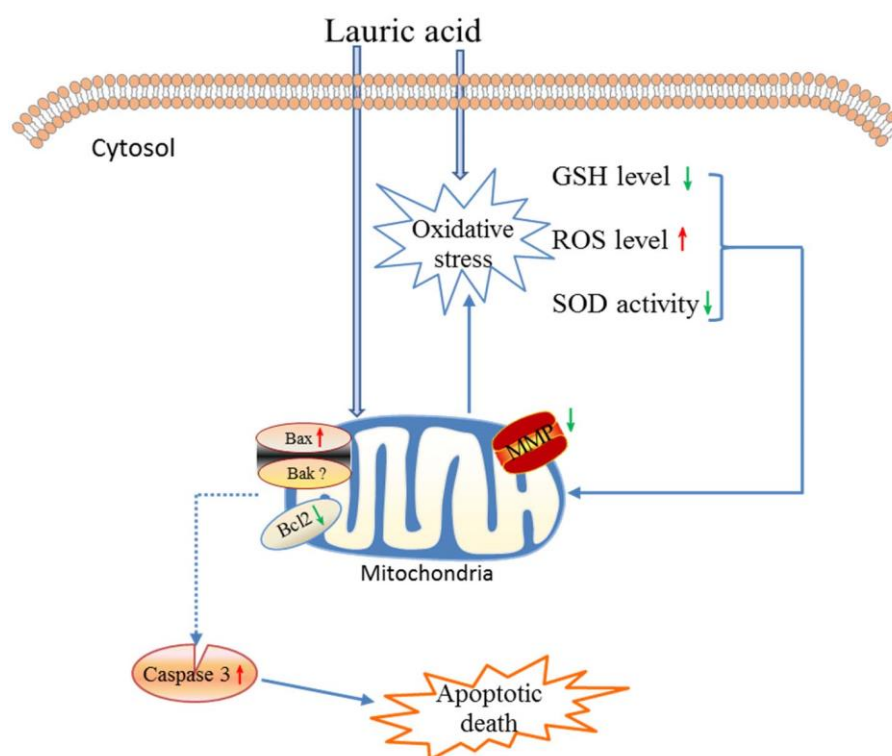


Figure 9. Schematic representation of the possible pathway of DDA-induced death in liver tumor cells. DDA perturbs redox balance and causes oxidative stress, leading to the functional destruction of mitochondria. Dysfunctional mitochondria generate more ROS and less GSH while decreasing SOD activity, which further causes the production of more ROS, thus resulting in positive feedback during oxidative stress. Overall, enhanced oxidative stress (i.e., increased ROS levels) and mitochondrial dysfunction contribute to cell death.

Authors' Contributions: The authors make the following contributions to the paper: study conception and design: CHEN, X.; data collection: LV, Q.; analysis and interpretation of results: LI, H.; draft manuscript preparation: CHEN, X., WANG, Z. All authors reviewed the results and approved the final version of the manuscript.

Conflicts of Interest: The authors declare that they have no conflicts of interest to report regarding the present study.

Ethics Approval: All experiments and methods were performed in accordance with the relevant approved guidelines and regulations, as well as under the approval of the Medical Ethics Committee of the First Affiliated Hospital of Henan University of Science and Technology (ID Number: 4103050043305) prior to commencing this study.

Acknowledgments: We would like to acknowledge all coordinators involved in this study. This research was supported by Horizontal project funded by enterprises in Henan Province (No. 20240033).

References

- ANGELOVA, P.R. and ABRAMOV, A.Y. Role of mitochondrial ROS in the brain: from physiology to neurodegeneration. *FEBS letter*. 2018, **592**(5), 692-702. <https://doi.org/10.1002/1873-3468.1296>
- ANWANWAN, D. et al. Challenges in liver cancer and possible treatment approaches. *Biochimica et biophysica acta. Reviews on cancer*. 2020, **1873**(1), 188314. <https://doi.org/10.1016/j.bbcan.2019.188314>
- BERGSSON, G. et al. Killing of Gram-positive cocci by fatty acids and monoglycerides. *APMIS*. 2001, **109**(10), 670-678. <https://doi.org/10.1034/j.1600-0463.2001.d01-131.x>
- CAI, L. et al. Comparison of Cytotoxicity Evaluation of Anticancer Drugs between Real-Time Cell Analysis and CCK-8 Method. *ACS Omega*. 2019, **4**(7), 12036-12042. <https://doi.org/10.1021/acsomega.9b01142>
- CAO, Y. et al. The use of proteomic technologies to study molecular mechanisms of multidrug resistance in cancer. *European Journal of Medicinal Chemistry*. 2019, **15**, 423-434. <https://doi.org/10.1016/j.eimech.2018.10.001>
- COLOMBO, M. and LLEO, A. Refining surgical therapy of liver cancer in cirrhosis: etiology makes the difference. *Translational gastroenterology and hepatology*. 2018, **3**, 104. <https://doi.org/10.21037/tgh.2018.12.03>
- Conceição, L.L. Difference in fatty acids composition of breast adipose tissue in women with breast cancer and benign breast disease. *Nutrition Hospital*. 2016, **33**(6), 1354-1360. <https://doi.org/10.20960/nh.795>
- COWPPLI-BONY, A. et al. Descriptive epidemiology of cancer in metropolitan France: Incidence, survival and prevalence. *Bulletin du cancer*. 2019, **106**(7-8), 617-634. <https://doi.org/10.1016/j.bulcan.2018.11.016>
- DANIEL, P.T. Dissecting the pathways to death. *Leukemia*. 2000, **14**(12), 2035-2044. <https://doi.org/10.1038/sj.leu.2401940>
- DE CARVALHO, C.C.C.R. and Caramujo, M.J. The Various Roles of Fatty Acids. *Molecules*. 2018, **23**(10), 2583. <https://doi.org/10.3390/molecules23102583>
- DE MATTEIS, V. et al. Encapsulation of thermo-sensitive lauric acid in silica shell: a green derivate for chemo-thermal therapy in breast cancer cell. *Molecules*. 2019, **24**(11), 2034. <https://doi.org/10.3390/molecules24112034>
- DEVI, A. and KHATKAR B.S. Effects of fatty acids composition and microstructure properties of fats and oils on textural properties of dough and cookie quality. *Journal of Food Science And Technology*. 2018, **55**(1), 321-30. <https://doi.org/10.1007/s13197-017-2942-8>
- EDLICH, F. BCL-2 proteins and apoptosis: Recent insights and unknowns. *Biochemical and Biophysical Research Communications*. 2018, **500**(1), 26-34. <https://doi.org/10.1016/j.bbrc.2017.06.190>
- EYRES, L. et al. Coconut oil consumption and cardiovascular risk factors in humans. *Nutrition Review*. 2016, **74**(4), 267-280. <https://doi.org/10.1093/nutrit/nuw002>
- FAUSER, J.K. et al. Fatty acids as potential adjunctive colorectal chemotherapeutic agents. *Cancer Biology Therapy*. 2011, **11**(8), 724-731. <https://doi.org/10.4161/cbt.11.8.15281>
- FU, J. and WANG, H. Precision diagnosis and treatment of liver cancer in China. *Cancer Letter*. 2018, **412**, 283-288. <https://doi.org/10.1016/j.canlet.2017.10.008>
- GABBIA, D., CANNELLA, L. and DE MARTIN, S. The Role of Oxidative Stress in NAFLD-NASH-HCC Transition-Focus on NADPH Oxidases. *Biomedicines*. 2021, **9**(6), 687. <https://doi.org/10.3390/biomedicines9060687>
- GALLUZZI, L. et al. Methods for the assessment of mitochondrial membrane permeabilization in apoptosis. *Apoptosis*. 2007, **12**(5), 803-813. <https://doi.org/10.1007/s10495-007-0720-1>
- GAO, Q. et al. How chemotherapy and radiotherapy damage the tissue: Comparative biology lessons from feather and hair models. *Experimental dermatology*. 2019, **28**(4), 413-418. <https://doi.org/10.1111/exd.13846>
- HE, F., SHA Y. and WANG, B. Relationship between alcohol consumption and the risks of liver cancer, esophageal cancer, and gastric cancer in China: Meta-analysis based on case-control studies. *Medicine (Baltimore)*. 2021, **100**(33), e26982. <https://doi.org/10.1097/MD.00000000000026982>
- JIAO, G.Y., ZHOU, C.L. and SUN, C.H. Effect of medium-chain fatty acid complex and linoleic acid on chemotherapeutic efficacy of multiple cellular spheroids of ovarian cancer. *Chinese J Clinical Nutrition*. 2008, **16**(2), 85-88.

- KIRKIN, V., JOOS, S. And ZÖRNIG, M. The role of Bcl-2 family members in tumorigenesis. *Biochimica Et Biophysica Acta*. 2004, **1644**(2-3), 229-249. <https://doi.org/10.1016/j.bbamcr.2003.08.009>
- KONO, H. Protective effects of medium-chain triglycerides on the liver and gut in rats administered endotoxin. *Annals of Surgery*. 2003, **237**, 246-255. <https://doi.org/10.1097/01.SLA.0000048450.44868.B1>
- LAPPANO, R. et al. The lauric acid-activated signaling prompts apoptosis in cancer cells. *Cell Death Discovery*. 2017, **3**, 17063. <https://doi.org/10.1038/cddiscovery.2017.63>
- LIU, M.Y. et al. Effect of dietary supplementation with glycerol monolaurate on growth performance, digestive ability and chicken nutritional components of broilers. *Food Science*. 2018, **39**(15), 67-71.
- MORI, T. et al. Giving combined medium-chain fatty acids and glucose protects against cancer-associated skeletal muscle atrophy. *Cancer Science*. 2019, **110**(10), 3391-3399. <https://doi.org/10.1111/cas.14170>
- NARAYANAN, A. et al. Anticarcinogenic properties of medium chain fatty acids on human colorectal, skin and breast cancer cells in vitro. *International Journal of Molecular Sciences*. 2015, **16**(3), 5014-5027. <https://doi.org/10.3390/ijms16035014>
- NIA, A. and DHANASEKARAN R. Genomic Landscape of HCC. *Current hepatology reports*. 2020, **19**(4), 448-461. <https://doi.org/10.1007/s11901-020-00553-7>
- OKA, S. et al. A correlation of reactive oxygen species accumulation by depletion of superoxide dismutases with age-dependent impairment in the nervous system and muscles of Drosophila adults. *Biogerontology*. 2015, **16**(4), 485-501. <https://doi.org/10.1007/s10522-015-9570-3>
- PALIKARAS, K., LIONAKI, E. and TAVERNARAKIS, N. Mitophagy: In sickness and in health. *Molecular Cellular Oncology*. 2015, **3**(1), e1056332. <https://doi.org/10.1080/23723556.2015.1056332>
- PANTH, N., ABBOTT, K.A., DIAS, C.B., WYNNE, K. and GARG, M.L. Differential effects of medium- and long-chain saturated fatty acids on blood lipid profile: a systematic review and meta-analysis. *The American journal of clinical nutrition*. 2018, **108**(4), 675-687. <https://doi.org/10.1093/ajcn/nqy167>
- PETERSEN, M.C. and SHULMAN, G.I. Mechanisms of Insulin Action and Insulin Resistance. *Physiological reviews*. 2018, **98**(4), 2133-2223. <https://doi.org/10.1152/physrev.00063.2017>
- POLYZOS, S.A., KOUNTOURAS, J. and MANTZOROS, C.S. Obesity and nonalcoholic fatty liver disease: From pathophysiology to therapeutics. *Metabolism*. 2019, **92**, 82-97. <https://doi.org/10.1016/j.metabol.2018.11.014>
- RANGEL-SOSA, M.M., AGUILAR-CÓRDOVA, E. and ROJAS-MARTÍNEZ, A. Immunotherapy and gene therapy as novel treatments for cancer. *Colombia médica (Cali)*. 2017, **48**(3), 138-147. <https://doi.org/10.25100/cm.v48i3.2997>
- RIAL, E. et al. Lipotoxicity, fatty acid uncoupling and mitochondrial carrier function. *Biochimica et biophysica acta*. 2010, **1797**(6-7), 800-806. <https://doi.org/10.1016/j.bbabi.2010.04.001>
- SANKARAMAN, S. and SFERRA, T.J. Are we going nuts on coconut oil? *Current Nutrition Reports*. 2018, **7**(3), 107-115. <https://doi.org/10.1007/s13668-018-0230-5>
- SANTOS, H.O. et al. oil intake and its effects on the cardiometabolic profile-A structured literature review. *Progress In Cardiovascular Diseases*. 2019, **62**(5), 436-443. <https://doi.org/10.1016/j.pcad.2019.11.001>
- SCHWAB, U.S. et al. Lauric and palmitic acid-enriched diets have minimal impact on serum lipid and lipoprotein concentrations and glucose metabolism in healthy young women. *Journal of Nutrition*. 1995, **125**(3), 466-473. <https://doi.org/10.1093/jn/125.3.466>
- SHEELA, D.L., NARAYANANKUTTY, A., NAZEEM, P.A., RAGHAVAMENON, A.C. and MUTHANGAPARAMBIL, S.R. Lauric acid induces cell death in colon cancer cells mediated by the epidermal growth factor receptor downregulation: An in silico and in vitro study. *Human & Experimental Toxicology*. 2019, **38**(7), 753-761. <https://doi.org/10.1177/0960327119839185>
- SILVA M.O.D. et al. Development of a promising antitumor compound based on rhodium (ii) succinate associated with iron oxide nanoparticles coated with lauric acid/albumin hybrid: synthesis, colloidal stability and cytotoxic effect in breast carcinoma cells. *Journal of Nanoscience and Nanotechnology*. 2018, **18**(6), 3832-3843. <https://doi.org/10.1166/jnn.2018.15021>
- STAMENKOVIC, A. et al. Overcoming the bitter taste of oils enriched in fatty acids to obtain their effects on the heart in health and disease. *Nutrients*. 2019, **11**(5), 1179. <https://doi.org/10.3390/nu11051179>
- ST-ONGE, M.P. et al. Medium chain triglyceride oil consumption as part of a weight loss diet does not lead to an adverse metabolic profile when compared to olive oil. *Journal of the American College of Nutrition*. 2008, **27**(5), 547-552. <https://doi.org/10.1080/07315724.2008.10719737>
- UNGER, R.H. Lipotoxic diseases. *Annual review of medicine*. 2002, **53**, 319-336. <https://doi.org/10.1146/annurev.med.53.082901.104057>

VEERESH, BABU, S.V. et al. Lauric acid and myristic acid prevent testosterone induced prostatic hyperplasia in rats. *European Journal of Pharmacology*. 2010, **626** (2-3), 262-265. <https://doi.org/10.1016/j.ejphar.2009.09.037>

VIGILANZA P. et al. Modulation of intracellular glutathione affects adipogenesis in 3T3-L1 cells. *Journal of Cell Physiology*. 2011, **226**(8), 2016-24. <https://doi.org/10.1002/jcp.22542>

WU, D. et al. Hesperetin induces apoptosis of esophageal cancer cells via mitochondrial pathway mediated by the increased intracellular reactive oxygen species. *Tumour Biology*. 2016, **37**(3), 3451-3459. <https://doi.org/10.1007/s13277-015-4176-6>

XIAO, S. et al. Novel panaxadiol triazole derivatives induce apoptosis in HepG-2 cells through the mitochondrial pathway. *Bioorganic Chemistry*. 2020, **102**, 104078. <https://doi.org/10.1016/j.bioorg.2020.104078>

YANG, J. et al. Oxidative stress and cell cycle arrest induced by short-term exposure to dustfall PM (2.5) in A549 cells. *Environmental Science & Pollution Research*. 2015, **25**(23), 22408-22419. <https://doi.org/10.1007/s11356-017-0430-3>

ZEIGER, K. Lauric acid as feed additive- an approach to reducing *Campylobacter* spp. in broiler meat. *PLoS One*. 2017, **12**(4), e0175693. <https://doi.org/10.1371/journal.pone.0175693>

Received: 16 October 2023 | **Accepted:** 27 May 2024 | **Published:** 17 July 2024



This is an Open Access article distributed under the terms of the Creative Commons Attribution License, which permits unrestricted use, distribution, and reproduction in any medium, provided the original work is properly cited.